DALTON

Ruthenium(II) complexes of some new polynucleating ligands incorporating terpyridyl and macrocyclic aza-crown binding sites

Brenda Whittle, Stuart R. Batten, John C. Jeffery, Leigh H. Rees and Michael D. Ward *

School of Chemistry, University of Bristol, Cantock's Close, Bristol BS8 1TS, UK

A series of five new compounds has been prepared in which terpyridyl fragments are linked to hexadentate aza-crown macrocycles. Reaction of 1-aza-18-crown-6 (1,4,7,10,13-pentaoxa-16-azacyclooctadecane) and 1,10-diaza-18-crown-6 (1,4,10,13-tetraoxa-7,16-diazacyclooctadecane) with 4′-bromo-2,2′:6′,2″-terpyridine afforded macrocycles L^1–L^3 in which the aza-crown macrocycles are linked directly to the $C^{4'}$ position of the terpyridyl groups *via* the macrocyclic N atoms. Compounds L^1 and L^2 contain a single macrocycle (1-aza-18-crown-6 or 1,10-diaza-18-crown-6 respectively) attached to a terpyridyl group, whereas L^3 contains two terpyridyl groups attached to either end of a central 1,10-diaza-18-crown-6-unit. Alternatively, the aza-crown macrocycles reacted with 4′-[(4-bromomethyl)phenyl]terpyridine to give L^4 and L^5 in which the aza-crown fragments are separated from the terpyridyl fragments by tolyl spacers: L^4 contains one macrocycle attached to a terpyridyl core, whereas L^5 (like L^3) contains two terpyridyl binding sites attached to either end of a central 1,10-diaza-18-crown-6 unit. Reaction of these with $[Ru(terpy)Cl_3]$ afforded the complexes $[Ru(terpy)L^1][PF_6]_2$, $[Ru(terpy)L^2][PF_6]_2$, $[\{Ru(terpy)\}_2(\mu\text{-}L^3)][PF_6]_4$, $[Ru(terpy)(HL^4)][PF_6]_3$ and $[\{Ru(terpy)\}_2(\mu\text{-}H_2L^5)][PF_6]_6$, the last two having the aliphatic amine groups of the macrocycles protonated. The crystal structure of $[(terpy)Ru(L^2)Na(BF_4)_2][PF_6]\cdot 1.5Me_2CO$ {grown by recrystallising $[Ru(terpy)L^2][PF_6]_2$ from a medium containing traces of $NaBF_4$} shows that the pendant N_2O_4-donor macrocyclic group contains a sodium cation co-ordinated by five of the six macrocyclic donor atoms, and two additional monodentate BF_4^- ligands in axial positions. Significantly, the N atom of the macrocycle which is attached to the terpyridyl fragment is sp^2-hybridised with trigonal geometry, which permits the lone pair, in a p_z orbital, to conjugate with the π system of the terpyridyl fragment. This macrocylic amine group is therefore a poor base and is not co-ordinated to the sodium cation. The crystal structure of $[\{Ru(terpy)\}_2(\mu\text{-}H_2L^5)][PF_6]_6\cdot 2MeCN$ confirms that the central macrocycle is doubly protonated, with the extra protons inside the macrocyclic cavity consistent with an endocyclic disposition of lone pairs. The electrochemical and UV/VIS spectroscopic properties of the complexes were also examined: in the dinuclear complexes there is no electrochemical interaction between the remote metal centres across the saturated bridging group.

Ditopic ligands which contain a macrocyclic unit attached to another metal-ion binding site have found a very wide range of applications in numerous fields.[1] For example, where the macrocycle is attached to a polypyridyl unit, the resulting compounds can be used to prepare luminescent[2] or electrochemical[3] sensors in which the luminescence and/or redox properties of a metal–polypyridyl complex core is modified by co-ordination of Group I or II metal ions to peripheral crown-ether sites. Co-operative allosteric behaviour has also been demonstrated in such compounds, by taking advantage of the change in conformation of both the polypyridyl[4] and crown-ether[5] components of the ditopic ligand on co-ordination to a suitable metal ion: a change in the conformation of one component when bound to a metal ion affects the geometry and hence metal-binding ability of the secondary site. Photocatalysts have been prepared in which a nickel(II)-cyclam (1,4,8,11-tetraazacyclotetradecane) unit, a photocatalyst for CO_2 reduction, is covalently attached to a $\{Ru(bipy)_3\}^{2+}$-type sensitiser (bipy = 2,2′-bipyridine) *via* a ditopic ligand containing both cyclam and bipy binding sites,[6] and other ruthenium–polypyridyl/metal–cyclam complexes have been prepared using the same type of bridging ligand.[7] Mixed macrocyclic–polypyridyl compounds have also been used as effective ligands for selective metal-ion binding,[8] metal transport,[9] and even selective recognition of protonated diamines.[10]

We have been interested recently in studying the photochemical properties of polynuclear complexes which contain a luminescent chromophore [ruthenium(II)-, osmium(II)- or rhenium(I)-based] attached to a variety of quenching groups.[11] To extend the scope of these studies we have become interested in the extensive synthetic possibilities offered by the use of bridging ligands which contain a polypyridyl fragment (for the luminophore) attached to a macrocycle (for the quenching group), and describe here the preparation and some of the co-ordination behaviour of new compounds in which an aza-crown macrocycle is attached to a terpyridyl fragment (L^1, L^2 and L^4; Scheme 1), or two terpyridyl fragments are linked by a bridging aza-crown macrocycle (L^3 and L^5; Scheme 2). Aza-crown macrocycles are known to be effective ligands for lanthanides[12] as well as Group I and II metal ions[13] and transition metals,[14] so they have the potential to be used in a wide range of complexes. In addition L^3 and L^5 are new members of a popular class of bis-(terpyridyl) compounds which have the potential to be used in linear oligomers containing multiple redox-active and/or photochemically active units.[15,16]

Experimental

General details

Organic starting materials (including the aza-crown macrocycles) were obtained from Aldrich and used as received. Ruthenium(III) chloride hydrate was generously loaned by Johnson Matthey. Literature methods were used for the preparations of 4′-chloro-2,2′:6′,2″-terpyridine (cterpy),[15] 2,2′:6′,2″-terpyridin-4′(1′H)-one,[15] $[Ru(terpy)Cl_3]$,[17] and 4′-

[(4-bromomethyl)phenyl]terpyridine.[18] Instrumentation used for routine spectroscopic and electrochemical analyses has been described previously.[11]

Syntheses

4′-Bromo-2,2′:6′,2″-terpyridine (bterpy). 2,2′:6′,2″-Terpyridin-4′(1′H)-one (4.40 g, 17.7 mmol) was dissolved in a mixture of $POCl_3$ (50 cm^3), PBr_3 (50 cm^3) and $POBr_3$ (5 g). The mixture was heated to 100 °C with stirring for 7 d. After cooling the reaction mixture was carefully poured onto crushed ice with vigorous mixing and left for 1 h until the reaction was complete. The solution was then made basic by slow addition of aqueous NaOH. The resulting white precipitate was filtered off, washed well with water, and dried *in vacuo*. Proton NMR analysis of the crude mixture showed that it contained about 5% cterpy as a contaminant; it was purified by recrystallisation from ethanol to give bterpy in 60–70% yield [electron impact (EI) mass spectrum: m/z = 311/313]. The ^1H and ^{13}C NMR spectra were identical to those published.[19]

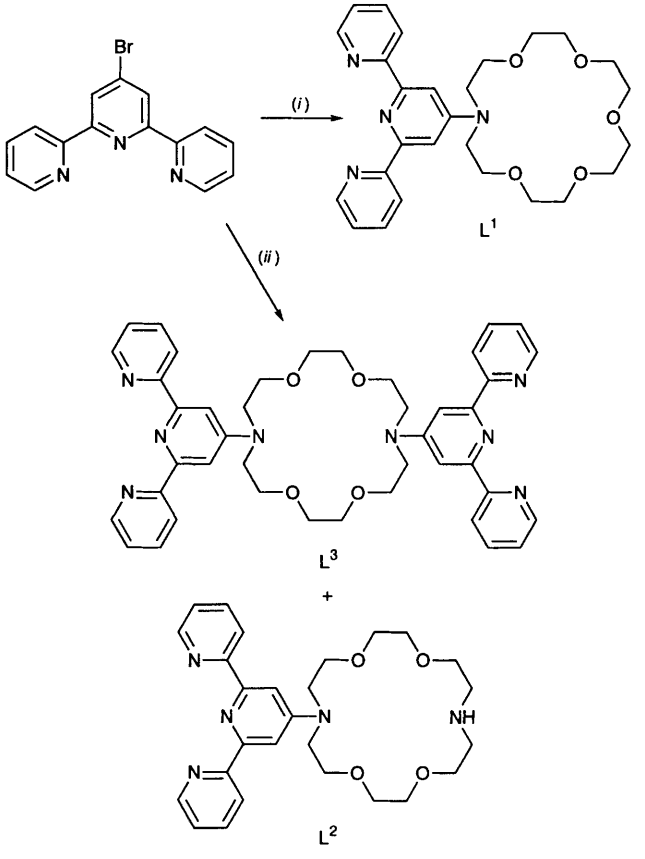

Scheme 1 Syntheses of L^1–L^3. (*i*) aza-18-crown-6 (1,4,7,10,13-pentaoxa-16-azacyclooctadecane), melt (160 °C); (*ii*) diaza-18-crown-6 (1,4,10,13-tetraoxa-7,16-diazacyclooctadecane), melt (160 °C)

L^1. An intimate mixture of aza-18-crown-6 (0.094 g, 0.36 mmol) and bterpy (0.1 g, 0.32 mmol) in a Schlenk tube under N_2 was heated at 160 °C for 18 h. The resulting brown tar was dissolved in CH_2Cl_2 and purified by preparative-scale thin-layer chromatography on 1.5 mm thick Al_2O_3 plates (Merck article 5726), using CH_2Cl_2–MeOH (98.5:1.5) as eluent. The major band (purple luminescence under 366 nm UV light) was scraped off and the product removed from the alumina by soaking in the eluent mixture. Evaporation of the resulting solution to dryness gave L^1 as a white waxy solid (0.085 g, 55%).

L^2. An intimate mixture of 1,10-diaza-18-crown-6 (0.084 g, 0.32 mmol) and bterpy (0.1 g, 0.32 mmol) in a Schlenk tube under N_2 was heated to 195 °C for 4 h. Work-up as above afforded a mixture of products: the slower-moving luminescent band on the TLC plate was L^2, which was isolated in 40% yield, and the faster-moving band was L^3 (below) isolated in trace amounts (< 10%). Both compounds are white, waxy solids.

L^3. An intimate mixture of 1,10-diaza-18-crown-6 (0.057 g, 0.22 mmol) and bterpy (0.15 g, 0.48 mmol) in a Schlenk tube under N_2 was heated to 190 °C for 20 h. Work-up as above afforded L^3 as a waxy solid (0.075 g, 47%).

L^4. A mixture of aza-18-crown-6 (0.205 g, 0.78 mmol), 4′-[(4-bromomethyl)phenyl]terpyridine (0.312 g, 0.78 mmol) and $NEtPr^i_2$ (0.7 cm^3, 3.9 mmol) in ethanol (20 cm^3) was heated to reflux for 1.5 h. Evaporation of the solvent *in vacuo* afforded an oil, which was purified by chromatography on an alumina column (Brockmann activity III) with CH_2Cl_2 containing 1% methanol to give pure L^4 as an oil in 80% yield.

L^5. A mixture of diaza-18-crown-6 (0.079 g, 0.30 mmol), 4′-[(4-bromomethyl)phenyl]terpyridine (0.249 g, 0.62 mmol) and

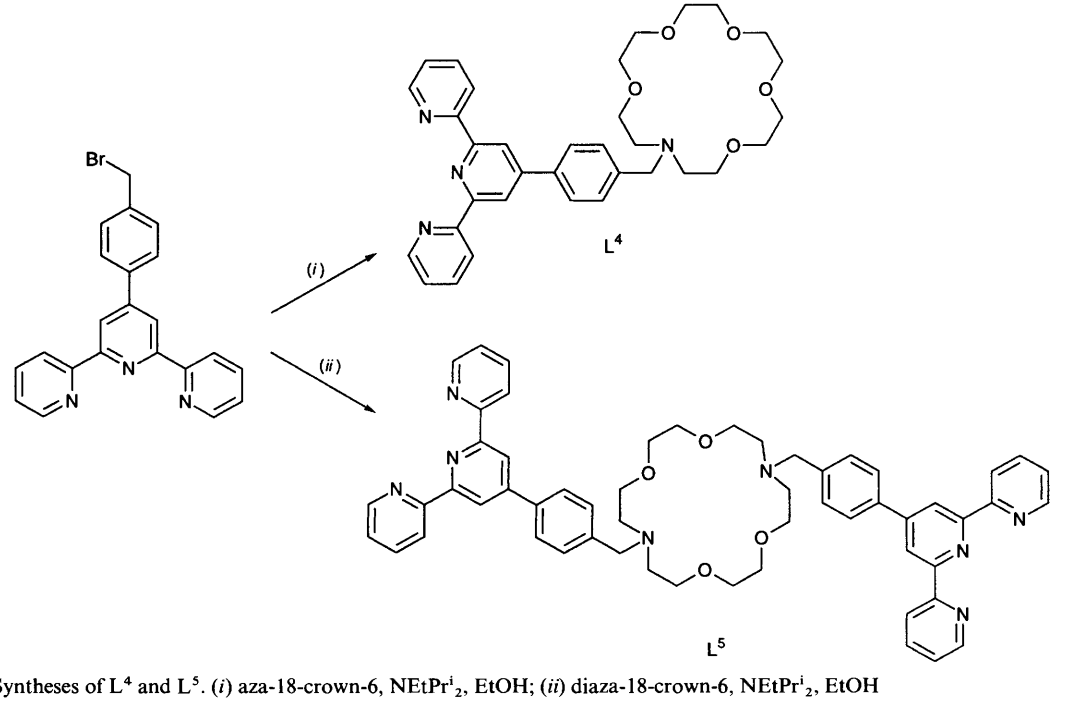

Scheme 2 Syntheses of L^4 and L^5. (*i*) aza-18-crown-6, $NEtPr^i_2$, EtOH; (*ii*) diaza-18-crown-6, $NEtPr^i_2$, EtOH

$NEtPr^i_2$ (0.7 cm^3, 3.9 mmol) in ethanol (15 cm^3) was heated to reflux for 1.5 h, after which time a precipitate had formed. After cooling (0 °C) the solid material was filtered off, washed with ethanol and then diethyl ether and dried, giving pure L^5 in 60% yield.

Characterisation data for L^1–L^5 are in Tables 1 and 2.

$[Ru(terpy)L^1][PF_6]_2$, $[Ru(terpy)L^2][PF_6]_2$, $[\{Ru(terpy)\}_2(\mu\text{-}L^3)][PF_6]_4$, $[Ru(terpy)(HL^4)][PF_6]_3$ and $[\{Ru(terpy)\}_2(\mu\text{-}H_2L^5)][PF_6]_6$. These ruthenium(II) complexes were all prepared in the same way. A mixture of the appropriate ligand (typically 0.2 mmol), 1.1 (for L^1, L^2 and L^4) or 2.2 (for L^3 and L^5) equivalents of $[Ru(terpy)Cl_3]$, and a few drops of *N*-methylmorpholine in MeOH (50 cm^3) was heated to reflux with stirring for 3 h. The orange mixture was then filtered to remove any solids, and treated with aqueous NH_4PF_6 to precipitate the complex which was filtered off and dried. The crude products were all purified by flash chromatography on silica as follows. For $[Ru(terpy)L^1][PF_6]_2$ initial elution was with MeCN–water–saturated aqueous KNO_3 (100:10:1) to remove low-polarity impurities, followed by the same mixture in proportions 100:10:3 which resulted in elution of the main red-orange band. For $[Ru(terpy)L^2][PF_6]_2$ and $[\{Ru(terpy)\}_2(\mu\text{-}H_2L^5)][PF_6]_6$ elution was with MeCN–water–saturated aqueous KNO_3 (14:2:1) throughout. For $[\{Ru(terpy)\}_2(\mu\text{-}L^3)][PF_6]_4$ initial elution was with acetone–saturated aqueous KNO_3 (10:3) to remove low-polarity impurities, followed by the same mixture in proportions 10:4 to elute the main band. For $[Ru(terpy)HL^4][PF_6]_3$ elution was with MeCN–water–saturated aqueous KNO_3 (100:10:5) throughout. In each case the central part of the main red-orange band was collected; the solutions were then reduced in volume until the organic part of the solvent mixture was removed, and the complexes were precipitated by addition of aqueous NH_4PF_6 and filtered off. To ensure complete removal of traces of KNO_3 and NH_4PF_6, the solids were dissolved in MeCN, an equal volume of water added, and the mixture concentrated *in vacuo* until the complex reprecipitated and was again filtered off, washed well with water, and dried. The yields were typically 30–50%. Characterisation data for the complexes are in Table 3.

Crystallography

Crystals of $[(terpy)Ru(L^2)Na(BF_4)_2][PF_6]\cdot 1.5Me_2CO$ were grown from acetone–ether, those of $[\{Ru(terpy)\}_2(\mu\text{-}H_2L^5)][PF_6]_6\cdot 2MeCN$ from acetonitrile–ether. Suitable crystals were coated in mineral oil and mounted on the diffractometer in a stream of cold N_2 (−100 °C) as quickly as possible to minimise decomposition from solvent loss.

Data were collected using a Siemens SMART three-circle diffractometer with a CCD area detector (graphite-monochromatised Mo-Kα X-radiation, $\bar{\lambda} = 0.710\,73$ Å). They were corrected for Lorentz-polarisation effects, and for absorption by an empirical method based on multiple measurements of equivalent data. Details of the crystal parameters, data collection and refinement are in Table 4. The structures were solved by conventional direct methods using SHELXTL and refined by the full-matrix least-squares method on all F^2 data with the SHELXTL 5.03 package using a Silicon Graphics Indy computer.[20] All non-hydrogen atoms were refined anisotropically; hydrogen atoms were included in calculated positions and refined with isotropic thermal parameters.

In $[(terpy)Ru(L^2)Na(BF_4)_2][PF_6]\cdot 1.5Me_2CO$ three solvent molecules occurred but with a 50% occupancy of each position. Two of them overlapped and shared two atoms [C(103) and C(104)] which were consequently refined with 100% site occupancy. The oxygen atoms could not be distinguished from the carbon atoms, so all solvent heavy atoms were refined as carbon atoms. In $[\{Ru(terpy)\}_2(\mu\text{-}H_2L^5)][PF_6]_6\cdot 2MeCN$ the complex molecule lies astride an inversion centre, so the asymmetric unit contains half of the complex, three hexafluorophosphate anions and one well behaved MeCN molecule. Selected bond lengths and angles for the two structures are in Tables 5 and 6.

Atomic coordinates, thermal parameters and bond lengths and angles have been deposited at the Cambridge Crystallographic Data Centre (CCDC). See Instructions for Authors, *J. Chem. Soc., Dalton Trans.*, 1996, Issue 1. Any request to the CCDC for this material should quote the full literature citation and the reference number 186/224.

Results and Discussion

Ligand syntheses

We used two different strategies for attaching aza-crown macrocycles to the terpyridyl fragments: direct attachment of the N atom of the macrocycle to a pyridyl ring using 4′-bromo-2,2′:6′,2″-terpyridine (L^1–L^3), and attachment *via* a tolyl spacer (L^4 and L^5) (Schemes 1 and 2). Attachment of aza-crown macrocycles to polypyridyl fragments is nearly always carried out by use of a polypyridyl fragment with a pendant CH_2X substituent, where X is a leaving group (halide, toluene-*p*-sulfonate); conventional displacement of X^- by the nucleophilic amine of the macrocycle under basic conditions results in a compound with a (polypyridyl)CH_2(macrocycle) construction, and L^4 and L^5 exemplify this more usual route.

We instead started by attaching the aza-crowns directly to terpyridyl fragments. This was prompted by the recent observation that NMe_2H reacts with 4′-chloro-2,2′:6′,2″-terpyridine (cterpy) in methanol at reflux to give 4′-(dimethylamino)terpyridine, provided the cterpy is first activated to nucleophilic attack by co-ordination to Fe^{II}.[21] Accordingly, we initially treated 1-aza-18-crown-6 with $[Fe(cterpy)_2]^{2+}$ at reflux in a variety of solvents; however, no reaction occurred, possibly because 1-aza-18-crown-6 is a poorer nucleophile than NMe_2H for steric reasons. We therefore tried instead a recently reported method in which aza-crowns were directly attached to 4,7-dichloro-1,10-phenanthroline in a high-temperature melt.[3] This proved to be quite straightforward, just requiring reaction of the appropriate macrocycle with 4′-bromo-2,2′:6′,2″-terpyridine (bterpy, a better electrophile than cterpy) as a high-temperature melt under N_2;[3] bterpy has been mentioned in several recent publications,[15,19] but full experimental information has not been given for its synthesis, so details are included in this paper.

Thus, reaction of 1-aza-18-crown-6 with 1 equivalent of bterpy afforded L^1; L^2 and L^3 were obtained by reaction of 1,10-diaza-18-crown-6 with 1 or 2 equivalents of bterpy respectively (Scheme 1). Use of solvents, and additional base to assist in deprotonation of the secondary amine group of the macrocycle, was not necessary. Scaling up the reactions decreased the yields somewhat, and we found that ≈100 mg scale reactions provided useful amounts of the ligands without compromising the yields too much: the moderate yields (40–50%) are compensated for by the simplicity of the reaction.

Compounds L^4 and L^5 were simply prepared in high yields by reaction of the appropriate aza-crown with 4′-[(4-bromomethyl)phenyl]terpyridine in ethanol at reflux, using $NEtPr^i_2$ as base (Scheme 2): this is a previously published general method for attaching aza-crowns to oligopyridines which have CH_2Br substituents.[9]

The identities of all five compounds were confirmed by ^1H and ^{13}C NMR spectroscopy (Table 1), mass spectrometry, and elemental analyses (Table 2).

Complex syntheses

The mononuclear complexes $[Ru(terpy)L^1][PF_6]_2$, $[Ru(terpy)L^2][PF_6]_2$ and $[Ru(terpy)HL^4][PF_6]_3$ were prepared

by reaction of the appropriate ligand with [Ru(terpy)Cl_3] in methanol. The reaction benefited considerably from addition of a few drops of the reducing agent *N*-methylmorpholine to the mixture, which assists in the reduction of Ru^{III} to Ru^{II} and affords much cleaner reaction mixtures. In the same way, reaction of L^3 or L^5 with 2 equivalents of [Ru(terpy)Cl_3] afforded the dinuclear complexes in which two $\{Ru(terpy)_2\}^{2+}$ chromophores are linked by a macrocyclic spacer group. The work-up involved chromatographic purification with a polar solvent mixture containing KNO_3. In order to avoid problems with occupation of the macrocyclic cavities by K^+ ions, the complexes were reprecipitated several times by addition of distilled water to MeCN solutions followed by filtration and drying.

The complexes were all characterised by elemental analyses {apart from [Ru(terpy)L^2][PF_6]$_2$, for which reliable data could not be obtained, see later} and either fast-atom bombardment (FAB) or electrospray (ES) mass spectrometry. The results showed that the complex with L^4 contains one extra HPF_6 formula unit to give [Ru(terpy)(HL^4)][PF_6]$_3$, and the dinuclear complex with L^5 contains two extra HPF_6 formula units to give [{Ru(terpy)}$_2$(μ-H_2L^5)][PF_6]$_6$. This may be ascribed to protonation of the macrocyclic amine groups, and the formulations reflect this (*i.e.* HL^4 and H_2L^5 as the bridging ligands). This does not occur for the complexes with L^1–L^3, indicating that the amine groups directly attached to the pyridine rings in these ligands are less basic than the aliphatic amines of L^4 and L^5.

Under the conditions of FAB mass spectra normally only species with a charge of 1+ were seen, corresponding either to loss of one hexafluorophosphate anion or gain of one sodium cation (probably by co-ordination into the macrocyclic cavity). Occasionally we also observed weak peaks for species that would be expected to have a 2+ charge, but at an *m/z* value corresponding to a 1+ charge. Thus [Ru(terpy)L^1]$^+$ (*m/z* 829) must arise from partial reduction of the dication under the FAB conditions. The ES mass spectra in contrast allowed a variety of differently charged species to be detected, both due to loss of hexafluorophosphate anions and the presence of protons on the macrocyclic amine, and in [{Ru(terpy)}$_2$(μ-H_2L^5)][PF_6]$_6$ for example the higher charge arising from the presence of the additional protons is quite clear. The ES mass spectra were particularly helpful for the dinuclear complexes with L^3 and L^5 which were too involatile to give good FAB spectra, and the technique has recently become very popular for characterisation of high-molecular-weight, highly charged co-ordination complexes which do not give good FAB spectra.[22]

Table 1 NMR data (δ, *J*/Hz) for the new ligands

	^{1}H (300 MHz, 293 K)*	^{13}C (75.45 MHz, 293 K)*
L^1	8.65 (2 H, ddd, J = 4.8, 1.8, 1.0, pyridyl H^6/H$^{6''}$), 8.60 (2 H, dt, J = 7.9, 1.0, pyridyl H^3/H$^{3''}$), 7.83 (2 H, td, J = 7.7, 1.8, pyridyl H^4/H$^{4''}$), 7.81 (2 H, s, pyridyl H$^{3'}$/H$^{5'}$), 7.31 (2 H, ddd, J = 6.1, 4.8, 1.1, pyridyl H^5/H$^{5''}$), 3.79 (8 H, m, CH_2), 3.64 (8 H, m, CH_2), 3.60 (8 H, m, CH_2)	157.3, 156.1, 155.1, 149.2, 136.9, 123.8, 121.5, 103.9, 71.2, 71.1, 71.0, 70.9, 68.7, 51.1
L^2	8.66 (2 H, m, pyridyl H^6/H$^{6''}$), 8.60 (2 H, d, J = 7.9, pyridyl H^3/H$^{3''}$), 7.81 (2 H, td, J = 7.7, 1.8, pyridyl H^4/H$^{4''}$), 7.79 (2 H, s, pyridyl H$^{3'}$/H$^{5'}$), 7.28 (2 H, ddd, J = 6.0, 4.8, 1.1, pyridyl H^5/H$^{5''}$), 3.91 (4 H, m, CH_2), 3.80 (4 H, m, CH_2), 3.63 (12 H, m, CH_2), 2.80 (4 H, m, CH_2), 2.45 (1 H, br s, NH)	157.0, 155.9, 154.6, 148.8, 136.6, 123.3, 121.3, 103.5, 70.5, 70.4, 70.3, 68.5, 50.0, 49.3
L^3	8.64 (4 H, ddd, J = 4.9, 1.7, 0.8, pyridyl H^6/H$^{6''}$), 8.59 (4 H, dt, J = 8.1, 1.0, pyridyl H^3/H$^{3''}$), 7.82 (4 H, td, J = 8.7, 2.0, pyridyl H^4/H$^{4''}$), 7.79 (4 H, s, pyridyl H$^{3'}$/H$^{5'}$), 7.30 (4 H, ddd, J = 6.0, 4.8, 1.1, pyridyl H^5/H$^{5''}$), 3.80 (16 H, m, CH_2), 3.69 (8 H, m, CH_2)	157.2, 156.1, 155.0, 149.2, 137.0, 123.8, 121.5, 103.9, 71.4, 69.1, 51.3
L^4	8.73 (2 H, s, pyridyl H$^{3'}$/H$^{5'}$), 8.71 (2 H, d, J = 4.5, pyridyl H^6/H$^{6''}$), 8.65 (2 H, d, J = 7.9, pyridyl H^3/H$^{3''}$), 7.85 (4 H, m, pyridyl H^4/H$^{4''}$ and aryl H^2/H^6), 7.48 (2 H, d, J = 8.2, aryl H^3/H^5), 7.33 (2 H, ddd, J = 7.4, 5.0, 1.3, pyridyl H^5/H$^{5''}$), 3.74 (2 H, s, tolyl CH_2), 3.66 (20 H, m, crown CH_2O), 2.83 (4 H, m, crown CH_2N)	156.2, 155.8, 150.1, 149.1, 149.0, 148.8, 136.9, 136.8, 129.4, 127.1, 123.8, 121.3, 118.7, 70.8, 70.7, 70.3, 69.9, 59.7, 53.9
L^5	8.72 (4 H, s, pyridyl H$^{3'}$/H$^{5'}$), 8.70 (4 H, m, pyridyl H^6/H$^{6''}$), 8.65 (4 H, dt, J = 7.9, 1.0, pyridyl H^6/H$^{6''}$), 7.85 (8 H, m, pyridyl H^4/H$^{4''}$ and aryl H^2/H^6), 7.49 (4 H, d, J = 8.3, aryl H^3/H^5), 7.31 (4 H, ddd, J = 7.5, 4.8, 1.3, pyridyl H^5/H$^{5''}$), 3.77 (4 H, s, tolyl CH_2), 3.65 (16 H, m, crown CH_2O), 2.88 (8 H, m, crown CH_2N)	155.2, 154.8, 149.0, 148.0, 139.9, 135.9, 135.8, 128.3, 126.1, 122.7, 120.3, 117.7, 69.7, 69.0, 58.7, 52.9

* The following solvents were used: L^1 and L^3, CD_2Cl_2; L^2, L^4 and L^5, $CDCl_3$.

Crystal structures

Repeated attempts to crystallise the complexes of L^1–L^3 were unsuccessful. Crystals of [Ru(terpy)L^1][PF_6]$_2$ were obtained but a combination of severe disorder in the flexible crown-ether unit and a large number of parameters (two independent molecules in the asymmetric unit) prevented a successful refinement. Accordingly we tried adding alkali-metal salts to the mixtures to see if they would be incorporated into the macrocycles and thus render them rigid. Crystallisation of [Ru(terpy)L^2][PF_6]$_2$ from acetone containing a small amount of $NaBF_4$ afforded crystals which were shown by crystallographic analysis to be [(terpy)Ru(L^2)Na(BF_4)$_2$][PF_6]·1.5Me_2CO (Fig. 1, Table 5). The co-ordination geometry of the {Ru(terpy)$_2$} core is unremarkable, but the pendant macrocyclic fragment has some interesting features. First, and most obviously, the sodium cation lies within the cavity, co-ordinated by all four oxygen atoms and one of the nitrogen atoms [N(80)] in an approximate plane. The deviations of these five donor

Table 2 Elemental analytical and mass spectral data for the new ligands

	Analysis (%)[a]			Principal mass spectral peaks
	C	H	N	*m/z*
L^1	65.3 (65.6)	6.8 (6.9)	11.3 (11.3)	494 (M^+)[b]
L^2	66.0 (65.7)	7.2 (7.2)	14.6 (14.2)	493 (M^+)[b]
L^3	69.1 (69.6)	5.9 (6.1)	15.4 (15.5)	747 ([M + Na]$^+$), 725 (M^+)[c]
L^4	69.3 (69.8)	7.1 (6.9)	9.5 (9.6)	584 (M^+)[b]
L^5	73.9 (74.3)	6.1 (6.3)	12.1 (12.4)	944 ([M + K]$^+$), 928 ([M + Na]$^+$)[c]

[a] Calculated values in parentheses. [b] Electron-impact mass spectrum. [c] Fast-atom bombardment mass spectrum.

Table 3 Analytical and mass spectroscopic data for the new complexes

Complex	Analysis (%)[a] C	H	N	Mass spectroscopic data *m/z*
$[Ru(terpy)L^1][PF_6]_2 \cdot 2H_2O$	43.6 (43.6)	4.1 (4.3)	8.7 (8.5)	1142 ($[M + Na]^+$), 974 ($[M - PF_6]^+$), 829 ($[M - 2PF_6]^+$)[b]
$[Ru(terpy)L^2][PF_6]_2$	*c*			1141 ($[M + Na]^+$), 1119 ($[M + H]^+$), 973 ($[M - PF_6]^+$)[b]
$[\{Ru(terpy)\}_2(\mu\text{-}L^3)][PF_6]_4$	43.0 (43.8)	3.5 (3.4)	9.9 (9.9)	842 ($[M - 2PF_6]^{2+}$), 513 ($[M - 3PF_6]^{3+}$), 348 ($[M - 4PF_6]^{4+}$)[d]
$[Ru(terpy)(HL^4)][PF_6]_3 \cdot MeCN$	43.9 (43.9)	4.2 (4.0)	8.3 (8.0)	1232 ($[M + Na]^+$), 1210 ($[M + H]^+$), 1088 ($[M + Na - PF_6]^+$), 1065 ($[M + H - PF_6]^+$), 919 ($[M - 2PF_6]^+$)[b]
$[\{Ru(terpy)\}_2(\mu\text{-}H_2L^5)][PF_6]_6$	42.5 (42.3)	3.3 (3.3)	8.1 (8.0)	622 ($[M + H - 2PF_6]^{3+}$), 573 ($[M - 3PF_6]^{3+}$), 430 ($[M + H - 3PF_6]^{4+}$), 393 ($[M - 4PF_6]^{4+}$), 315 ($[M + H - 4PF_6]^{5+}$)[d]

[a] Calculated values in parentheses. [b] FAB data. [c] Reliable elemental analysis could not be obtained; see text. [d] ES data.

Table 4 Crystallographic data for complexes $[(terpy)Ru(L^2)Na(BF_4)_2][PF_6] \cdot 1.5Me_2CO$ and $[\{Ru(terpy)\}_2(\mu\text{-}H_2L^5)][PF_6]_6 \cdot 2MeCN$

	$[(terpy)Ru(L^2)Na(BF_4)_2][PF_6] \cdot 1.5Me_2CO$	$[\{Ru(terpy)\}_2(\mu\text{-}H_2L^5)][PF_6]_6 \cdot 2MeCN$
Formula	$C_{46.5}H_{55}B_2F_{14}N_8NaO_{5.5}PRu$	$C_{90}H_{86}F_{36}N_{16}O_4P_6Ru_2$
M	1256.63	2527.71
System, space group	Triclinic, $P\bar{1}$	Monoclinic, $P2_1/c$
a/Å	8.813(2)	14.313(2)
b/Å	11.894(5)	22.862(3)
c/Å	15.107(4)	16.508(3)
α/°	108.76(2)	
β/°	97.58(3)	109.74(2)
γ/°	97.09(3)	
U/Å^3	1462.9(9)	5084.3(14)
Z	1	2
D_c/g cm^{-3}	1.426	1.651
μ/mm^{-1}	0.397	0.516
F(000)	640	2544
Crystal size/mm	0.40 × 0.30 × 0.15	0.40 × 0.40 × 0.20
2θ Range/°	5–50	4.4–50
Reflections collected (total, independent, R_{int})	7008, 5776, 0.021	23 769, 8945, 0.043
Data, restraints, parameters	5776, 3, 698	8945, 0, 699
Final *R*1, *wR*2[a,b]	0.0458, 0.1289	0.0569, 0.1653
Weighting factors (*a*, *b*)[b]	0.1008, 0.8864	0.0914, 1.7896
Largest peak, hole/e Å^{-3}	+0.762, −0.761	1.245, −0.603

[a] Structure was refined on F_o^2 using all data; the value of *R*1 is given for comparison with older refinements based on F_o with a typical threshold of $F \geqslant 4\sigma(F)$. [b] $wR2 = [\Sigma w(F_o^2 - F_c^2)^2/\Sigma w(F_o^2)^2]^{\frac{1}{2}}$ where $w^{-1} = [\sigma^2(F_o^2) + (aP)^2 + bP]$ and $P = [\max(F_o^2, 0) + 2F_c^2]/3$.

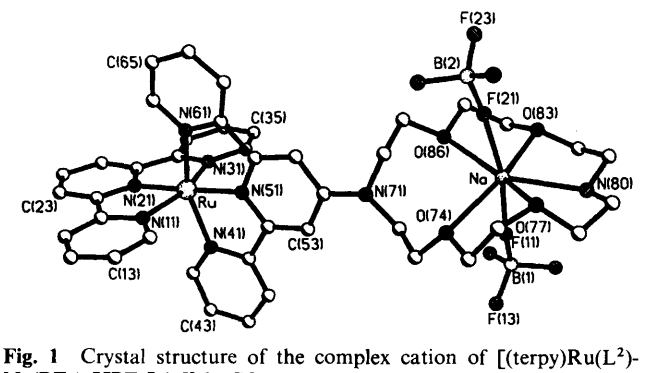

Fig. 1 Crystal structure of the complex cation of $[(terpy)Ru(L^2)Na(BF_4)_2][PF_6] \cdot 1.5Me_2CO$

atoms from the mean plane through them are as follows: O(74), −0.493; O(77), +0.691; N(80), −0.475; O(83), +0.060; O(86), +0.217 Å. The sodium atom lies just 0.015 Å out of the mean plane of these five donor atoms. The sodium–macrocycle bond distances lie in the range 2.41–2.53 Å which are typical of sodium complexes with other crown-ether macrocycles.[23] The sodium ion also has two monodentate BF_4^- ligands in axial positions either side of the macrocyclic ring. Secondly, the N atom which is attached to the pyridyl ring is trigonal planar, *i.e.* sp^2-hybridised so that the p_z orbital which formally contains the lone pair is directly conjugated with the aromatic pyridine ring.[20] The trigonal plane about N(71) is inclined at just 10° to the plane of the pyridyl ring to which it is attached, consistent with this suggestion. This aromatic nitrogen atom will therefore be less strongly basic than the other (aliphatic) nitrogen atom, which accounts for the fact that it is not co-ordinated to the sodium cation. This also explains why the complexes of L^1 and L^3, in which the macrocyclic N atoms are also directly attached to pyridyl rings, are not protonated, in contrast to the complexes with L^4 and L^5. The facility with which L^2 scavenges alkali-metal ions from its environment may in part account for the fact that we could not get a reliable elemental analysis of $[Ru(terpy)L^2][PF_6]_2$.

The crystal structure of the cation of $[\{Ru(terpy)\}_2(\mu\text{-}H_2L^5)][PF_6]_6 \cdot 2MeCN$ is in Fig. 2 (see also Table 6). This is a centrosymmetric structure with the inversion centre in the middle of the macrocycle. Again the co-ordination geometry within each $\{Ru(terpy)_2\}$ unit is unremarkable. The protons on the nitrogen atoms of the macrocycle were located during the final stages of the refinement and were subsequently included in calculated positions. They lie inside the macrocyclic cavity, indicating that the lone pairs of the tertiary N atoms are directed inwards. The molecule is not fully 'stretched out' but folded to a certain extent; the Ru • • • Ru separation is 21.23 Å.

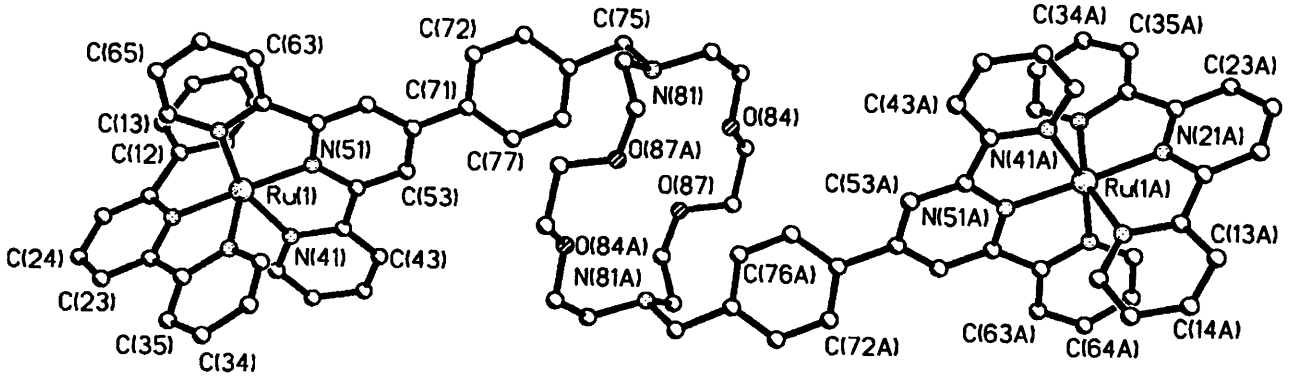

Fig. 2 Crystal structure of the complex cation of $[\{Ru(terpy)\}_2(\mu\text{-}H_2L^5)][PF_6]_6\cdot 2MeCN$

Electronic spectroscopy and electrochemistry

Electrochemical and electronic spectral data are summarised in Table 7. All of the complexes show the expected metal-centred oxidation and ligand-centred reductions. Except where stated otherwise in Table 7 all processes were chemically reversible with symmetric waves ($i_{p,a} = i_{p,c}$ at a scan rate of 0.2 V s^{-1}). For the complexes of L^1–L^3 the Ru^{II}–Ru^{III} couple is at a more cathodic potential than usual {*ca.* +0.5 V *vs.* ferrocene–ferrocenium, in contrast to +0.9 V for $[Ru(terpy)_2]^{2+}$} due to the presence of an electron-donating nitrogen substituent at the C^4 position of the central pyridyl ring of one of the ligands.[20] For the complexes of L^4 and L^5 in contrast the Ru^{II}–Ru^{III} couples revert to their usual values. The very strong electron-donating effect of the amine substituents in the complexes of L^1–L^3 is consistent with the sp^2 hybridisation that was apparent crystallographically, which allows the lone-pair orbital (p_z) to interact with the π system of the pyridyl ring. It also causes the ligand-based redox potentials to be rather cathodic compared to those of $[Ru(terpy)(HL^4)][PF_6]_3$ and $[\{Ru(terpy)\}_2(\mu\text{-}H_2L^5)][PF_6]_6$, since the excess of electron density on the metal centre will partly delocalise onto the terminal terpy ligands. For $[\{Ru(terpy)\}_2(\mu\text{-}L^3)][PF_6]_4$ and $[\{Ru(terpy)\}_2(\mu\text{-}H_2L^5)][PF_6]_6$ the two oxidations are (unsurprisingly) coincident, as are the terpy-based reductions.

The presence of the extra protons in the macrocyclic groups of $[Ru(terpy)(HL^4)][PF_6]_3$ and $[\{Ru(terpy)\}_2(\mu\text{-}H_2L^5)][PF_6]_6$ does not appear to have any significant effect on the electrochemistry, no doubt because it is the $\{Ru(terpy)_2\}^{2+}$

Table 5 Selected bond lengths (Å) and angles (°) for $[(terpy)Ru(L^2)Na(BF_4)_2][PF_6]\cdot 1.5Me_2CO$

Ru–N(21)	1.966(7)	Na–F(21)	2.295(5)
Ru–N(51)	2.004(7)	Na–F(11)	2.338(6)
Ru–N(31)	2.069(6)	Na–O(83)	2.406(6)
Ru–N(11)	2.071(5)	Na–N(80)	2.464(6)
Ru–N(41)	2.073(6)	Na–O(77)	2.465(5)
Ru–N(61)	2.078(5)	Na–O(74)	2.482(5)
		Na–O(86)	2.528(6)
N(21)–Ru–N(51)	178.1(3)	N(31)–Ru–N(41)	93.0(2)
N(21)–Ru–N(31)	79.2(3)	N(11)–Ru–N(41)	91.9(2)
N(51)–Ru–N(31)	100.8(3)	N(21)–Ru–N(61)	99.8(2)
N(21)–Ru–N(11)	78.9(3)	N(51)–Ru–N(61)	78.3(3)
N(51)–Ru–N(11)	101.1(3)	N(31)–Ru–N(61)	91.5(2)
N(31)–Ru–N(11)	158.2(2)	N(11)–Ru–N(61)	92.4(2)
N(21)–Ru–N(41)	103.4(2)	N(41)–Ru–N(61)	156.8(2)
N(51)–Ru–N(41)	78.5(3)		
F(21)–Na–F(11)	167.7(3)	F(11)–Na–O(74)	81.2(2)
F(21)–Na–O(83)	92.0(2)	O(83)–Na–O(74)	161.1(2)
F(11)–Na–O(83)	87.2(2)	N(80)–Na–O(74)	123.0(2)
F(21)–Na–N(80)	111.5(2)	O(77)–Na–O(74)	70.5(2)
F(11)–Na–N(80)	79.7(2)	F(21)–Na–O(86)	77.6(2)
O(83)–Na–N(80)	68.7(2)	F(11)–Na–O(86)	90.6(3)
F(21)–Na–O(77)	79.5(2)	O(83)–Na–O(86)	69.6(2)
F(11)–Na–O(77)	110.5(3)	N(80)–Na–O(86)	137.6(2)
O(83)–Na–O(77)	128.0(2)	O(77)–Na–O(86)	151.7(2)
N(80)–Na–O(77)	67.3(2)	O(74)–Na–O(86)	95.5(2)
F(21)–Na–O(74)	96.1(2)	C(54)–N(71)–C(72)	123.6(6)
C(54)–N(71)–C(88)	120.2(6)	C(72)–N(71)–C(88)	115.1(6)

Table 6 Selected bond lengths (Å) and angles (°) for $[\{Ru(terpy)\}_2(\mu\text{-}H_2L^5)][PF_6]_6\cdot 2MeCN$

Ru(1)–N(51)	1.975(4)	Ru(1)–N(11)	2.071(4)
Ru(1)–N(21)	1.978(4)	Ru(1)–N(41)	2.071(4)
Ru(1)–N(31)	2.061(4)	Ru(1)–N(61)	2.073(4)
C(80)–N(81)	1.488(8)	O(84)–C(85)	1.414(8)
C(80)–C(88A)	1.492(9)	C(85)–C(86)	1.504(10)
N(81)–C(82)	1.516(7)	C(86)–O(87)	1.388(7)
C(82)–C(83)	1.495(9)	O(87)–C(88)	1.423(8)
C(83)–O(84)	1.403(7)	C(88)–C(80A)	1.492(9)
N(51)–Ru(1)–N(21)	177.8(2)	N(31)–Ru(1)–N(41)	91.3(2)
N(51)–Ru(1)–N(31)	101.0(2)	N(11)–Ru(1)–N(41)	93.9(2)
N(21)–Ru(1)–N(31)	78.7(2)	N(51)–Ru(1)–N(61)	79.2(2)
N(51)–Ru(1)–N(11)	100.9(2)	N(21)–Ru(1)–N(61)	103.1(2)
N(21)–Ru(1)–N(11)	79.4(2)	N(31)–Ru(1)–N(61)	93.2(2)
N(31)–Ru(1)–N(11)	158.1(2)	N(11)–Ru(1)–N(61)	89.9(2)
N(51)–Ru(1)–N(41)	78.9(2)	N(41)–Ru(1)–N(61)	158.1(2)
N(21)–Ru(1)–N(41)	98.9(2)		

Table 7 Electrochemical and UV/VIS spectroscopic data for the new complexes

Complex	Electrochemical data[a] $E_{\frac{1}{2}}$/V (ΔE_p/mV)			UV/VIS spectral data (in MeCN) λ_{max}/nm ($10^{-3}\varepsilon$/dm^3 mol^{-1} cm^{-1})
$[Ru(terpy)L^1][PF_6]_2$	+0.50 (80)	−1.75 (70)	−2.04 (80)	493 (17), 309 (50), 299 (47), 272 (55), 233 (36)
$[Ru(terpy)L^2][PF_6]_2$	+0.53 (120)	−1.76 (90)	−2.04 (120)	493 (14), 309 (39), 300 (37), 272 (44), 234 (29)
$[\{Ru(terpy)\}_2(\mu\text{-}L^3)][PF_6]_4$	+0.56 (100)[b]	−1.79 (90)[b]	−2.01 (80)[b]	493 (40), 309 (102), 298 (99), 273 (116), 232 (83)
$[Ru(terpy)(HL^4)][PF_6]_3$	+0.90 (120)	−1.64 (90)	−1.89 (100)	484 (10), 308 (30), 283 (24)
$[\{Ru(terpy)\}_2(\mu\text{-}H_2L^5)][PF_6]_6$	+0.88 (110)[b]	−1.64 (110)[b]	−1.87[c]	484 (18), 308 (55), 283 (46)

[a] Electrochemical measurements were made in MeCN containing 0.1–0.2 mol dm^{-3} $NBu^n_4PF_6$ as base electrolyte at a Pt-bead working electrode with a scan rate of 0.2 V s^{-1}. Ferrocene was added as an internal standard at the end of each measurement, and all $E_{\frac{1}{2}}$ values are quoted in volts *vs.* the ferrocene–ferrocenium couple. [b] Two coincident one-electron processes. [c] Return wave obscured by desorption spike; the potential quoted is the peak of the outward scan.

centres that are the sites of all of the redox activity; the protonated amine groups of the macrocycle are insulated from them by CH_2 spacers. We note also that addition of salts of Group IA and IIA cations (up to a 10-fold excess compared to the ruthenium complex) to the electrochemical cell did not give significant shifts in any of the redox potentials for any of the complexes.

The electronic spectra of the complexes show a few points of interest. First, the spectra of the dinuclear complexes (with L^3 and L^5) are roughly double the intensity of those of their mononuclear analogues. The complexes with L^1–L^3 have λ_{max} for the characteristic $Ru(d_\pi) \rightarrow ligand(\pi^*)$ transition at a slightly lower energy (493 nm) than those of L^4 and L^5 (484 nm), as the π-donor effect of the amine substituent weakens the ligand field slightly and thereby raises the metal d_π levels.

Conclusion

We have prepared a variety of new terpyridine-based compounds in which aza-crown macrocycles are attached to the terpy fragment, either directly or *via* a tolyl spacer. These should prove to be versatile new ligands for a variety of applications in the areas of supramolecular photochemistry and high-nuclearity co-ordination chemistry. Some obvious areas for further development include: (*i*) insertion of luminescent lanthanide ions into the macrocyclic cavities of the ruthenium complexes, which will give complexes with two (potentially interacting) luminescent units; (*ii*) preparation of linear oligomers with the bridging L^3 and L^5, the properties of which such as one-dimensional conductivity may be modulated by the presence or absence of ions in the macrocyclic cavities. These areas are currently under investigation.

Acknowledgements

We thank the EPSRC for a postgraduate studentship (to B. W.), Miss Kate Byrom for recording the electrospray mass spectra, Dr. Ken MacNeil for recording the FAB mass spectra and Dr. Alex Cargill Thompson for assistance in preparing 4′-[(4-bromomethyl)phenyl]terpyridine and 4-bromoterpyridine.

References

1 F. C. J. M. van Veggel, W. Verboom and D. N. Reinhoudt, *Chem. Rev.*, 1994, **94**, 279.
2 P. D. Beer, O. Kocian, R. J. Mortimer and C. Ridgway, *J. Chem. Soc., Chem. Commun.*, 1991, 1460; O. Kocian, R. J. Mortimer and P. D. Beer, *J. Chem. Soc., Perkin Trans. 1*, 1990, 3203; P. D. Beer, O. Kocian, R. J. Mortimer and C. Ridgway, *Analyst (London)*, 1992, **117**, 1247.
3 M. Schmittel, H. Ammon and C. Wöhrle, *Chem. Ber.*, 1995, **128**, 845; M. Schmittel and H. Ammon, *J. Chem. Soc., Chem. Commun.*, 1995, 687.
4 P. D. Beer and A. S. Rothin, *J. Chem. Soc., Chem. Commun.*, 1988, **7**, 137; *Polyhedron*, 1988, **7**, 137.
5 J. R. Rebek, *Acc. Chem. Res.*, 1984, **17**, 258; T. Nabeshima, T. Inaba, T. Sagae and N. Furukawa, *Tetrahedron Lett.*, 1990, **31**, 3919; A. Gourdon, *New. J. Chem.*, 1992, **16**, 953; P. D. Beer, Z. Chan, A. Grieve and J. Haggitt, *J. Chem. Soc., Chem. Commun.*, 1994, 2413.
6 E. Kimura, X. Bu, M. Shionoya, S. Wada and S. Maruyama, *Inorg. Chem.*, 1992, **31**, 4542; E. Kimura, S. Wada, M. Shionoya and T. Takahashi, *J. Chem. Soc., Chem. Commun.*, 1990, 397; E. Fujita, J. J. Milder and B. S. Brunschwig, *Inorg. Chem.*, 1992, **31**, 2079.
7 S. C. Rawle, P. Moore and N. W. Alcock, *J. Chem. Soc., Chem. Commun.*, 1992, 684.
8 H. Tsukube, T. Hamada, T. Tanaka and J. Uenishi, *Inorg. Chim. Acta*, 1993, **214**, 1; C. F. Martens, R. J. M. Klein Gebbink, M. C. Feiters, H. Koojiman, W. J. J. Smeets, A. L. Spek and R. J. M. Nolte, *Inorg. Chem.*, 1994, **33**, 5541; D. Wang, H. Xiang, G. Wang, Z. Han, X. Yang, H. Hu and K. Yu, *J. Chem. Soc., Dalton Trans.*, 1994, 3325.
9 H. Tsukube, J. Uenishi, H. Higaki, K. Kikkawa, T. Tanaka, S. Wakabayashi and S. Oae, *J. Org. Chem.*, 1993, **58**, 4389.
10 M. S. Goodman, V. Jubian, B. Linton and A. D. Hamilton, *J. Am. Chem. Soc.*, 1995, **117**, 11610.
11 V. Balzani, D. A. Bardwell, F. Barigelletti, R. L. Cleary, M. Guardigli, J. C. Jeffery, T. Sovrani and M. D. Ward, *J. Chem. Soc., Dalton Trans.*, 1995, 3601; D. A. Bardwell, F. Barigelletti, R. L. Cleary, L. Flamigni, M. Guardigli, J. C. Jeffery and M. D. Ward, *Inorg. Chem.*, 1995, **34**, 2438; A. J. Amoroso, A. Das, J. A. McCleverty, M. D. Ward, F. Barigelletti and L. Flamigni, *Inorg. Chim. Acta*, 1994, **226**, 171; M. Guardigli, L. Flamigni, F. Barigelletti, C. S. W. Richards and M. D. Ward, *J. Phys. Chem.*, 1996, **100**, 10620.
12 F. Arnand-Neu, *Chem. Soc. Rev.*, 1994, 235; F. Nicolò, D. Plancherel, G. Chapuis and J.-C. G. Bünzli, *Inorg. Chem.*, 1988, **27**, 3518; F. Arnand-Neu, E. L. Loufouilou and M. J. Schwing-Weil, *J. Chem. Soc., Dalton Trans.*, 1986, 2629; J.-C. G. Bünzli, G. A. Leonard, D. Plancherel and G. Chapuis, *Helv. Chim. Acta*, 1986, **69**, 288.
13 F. Vögtle and E. Weber (Editors), *Host Guest Complex Chemistry – Macrocycles*, Springer, Berlin, 1985.
14 L. F. Lindoy, in *Synthesis of Macrocycles: The Design of Selective Complexing Agents*, eds. R. M. Izatt and J. J. Christensen, Wiley, New York, 1987, ch. 2.
15 E. C. Constable and M. D. Ward, *J. Chem. Soc., Dalton Trans.*, 1990, 1405.
16 G. D. Storrier and S. B. Colbran, *J. Chem. Soc., Dalton Trans.*, 1996, 2185; J.-P. Sauvage, J.-P. Collin, J.-C. Chambron, S. Guillerez, C. Coudret, V. Balzani, F. Barigelletti, L. De Cola and L. Flamigni, *Chem. Rev.*, 1994, **94**, 993; V. Grosshenny, A. Harriman and R. Ziessel, *Angew. Chem., Int. Ed. Engl.*, 1995, **34**, 2705; E. C. Constable, A. M. W. Cargill Thompson, P. Harveson, L. Macko and M. Zehnder, *Chem. Eur. J.*, 1995, **1**, 360; E. C. Constable and A. M. W. Cargill Thompson, *J. Chem. Soc., Dalton Trans.*, 1992, 3467.
17 B. P. Sullivan, J. M. Calvert and T. J. Meyer, *Inorg. Chem.*, 1980, **19**, 1404.
18 J.-P. Collin, S. Guillerez, J.-P. Sauvage, F. Barigelletti, L. De Cola, L. Flamigni and V. Balzani, *Inorg. Chem.*, 1991, **30**, 4230.
19 P. Péchy, F. P. Rotzinger, M. K. Nazeeruddin, O. Kohle, S. M. Zakeeruddin, R. Humphry-Baker and M. Grätzel, *J. Chem. Soc., Chem. Commun.*, 1995, 65; V. Grosshenny and R. Ziessel, *J. Organomet. Chem.*, 1993, **453**, C19.
20 SHELXTL 5.03 program system, Siemens Analytical X-Ray Instruments, Madison, WI, 1995.
21 E. C. Constable, A. M. W. Cargill Thompson, D. A. Tocher and M. D. Daniels, *New. J. Chem.*, 1992, **16**, 855.
22 M. Przybylski and M. O. Glocker, *Angew. Chem., Int. Ed. Engl.*, 1996, **35**, 807.
23 M. A. Bush and M. R. Truter, *J. Chem. Soc., Perkin Trans. 2*, 1972, 341; M. Dobler, J. D. Dunitz and P. Seiler, *Acta Crystallogr., Sect. B*, 1974, **30**, 2741.

Received 11*th June* 1996; *Paper* 6/04110H